

High voltage pulser for ion shutters in ion mobility spectrometry based on an optocoupler

Cite as: Rev. Sci. Instrum. **93**, 074703 (2022); <https://doi.org/10.1063/5.0093479>

Submitted: 29 March 2022 • Accepted: 14 June 2022 • Published Online: 12 July 2022

 Nattapong Chantipmanee, Marc-Aurèle Boillat and  Peter C. Hauser



View Online



Export Citation



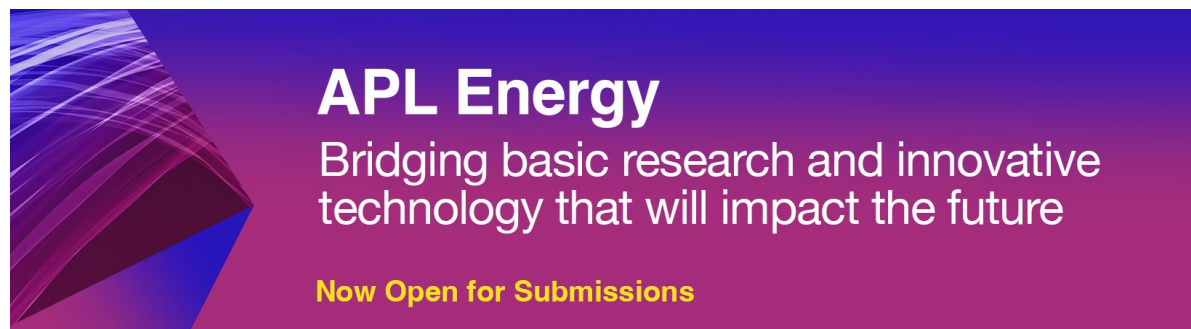
CrossMark

ARTICLES YOU MAY BE INTERESTED IN

[The ultrafast pixel array camera system and its applications in high energy density physics](#)
Review of Scientific Instruments **93**, 074702 (2022); <https://doi.org/10.1063/5.0091824>

[Design and performance of a nano-Newton torsion balance](#)
Review of Scientific Instruments **93**, 074502 (2022); <https://doi.org/10.1063/5.0086975>

[FPGA-based electronic system for the control and readout of superconducting quantum processors](#)
Review of Scientific Instruments **93**, 074701 (2022); <https://doi.org/10.1063/5.0085467>



APL Energy
Bridging basic research and innovative
technology that will impact the future
Now Open for Submissions

High voltage pulser for ion shutters in ion mobility spectrometry based on an optocoupler

Cite as: *Rev. Sci. Instrum.* **93**, 074703 (2022); doi: [10.1063/5.0093479](https://doi.org/10.1063/5.0093479)

Submitted: 29 March 2022 • Accepted: 14 June 2022 •

Published Online: 12 July 2022



View Online



Export Citation



CrossMark

Nattapong Chantipmanee,  Marc-Aurèle Boillat, and Peter C. Hauser^{a)} 

AFFILIATIONS

University of Basel, Department of Chemistry, Klingelbergstrasse 80, 4056 Basel, Switzerland

^{a)} Author to whom correspondence should be addressed: Peter.Hauser@unibas.ch

ABSTRACT

A novel high voltage pulser for an ion shutter used in drift-tube ion-mobility spectrometers is described. The simple design suitable for the in-house construction of these spectrometers relies on a special optocoupler to isolate the triggering circuitry from the high voltage at the ion shutter. The device was tested with an electrospray-ionization ion-mobility device with a 10 cm drift tube operated at 4 kV into which a standard test mixture of four tetraalkylamines was injected with a negative going gating pulse of about 50 V on top of 4 kV. A fall time of 15.7 μ s and a rise time of 2.0 μ s were determined for the pulse, which was adequate for the required injection pulse width of 450 μ s. Resolving powers between 61 and 81 were determined for the four quaternary amines, which were found to be comparable to the performance obtained with a previously reported pulser circuitry of a different design used as a reference.

© 2022 Author(s). All article content, except where otherwise noted, is licensed under a Creative Commons Attribution (CC BY) license (<http://creativecommons.org/licenses/by/4.0/>). <https://doi.org/10.1063/5.0093479>

I. INTRODUCTION

Ion mobility spectrometry (IMS) is an analytical technique in which ions are separated in a so-called drift tube in the gas phase by the application of an electric field.¹ It is an alternative to the separation techniques of chromatography and electrophoresis as well as to mass spectrometry. It is also used in combination with mass spectrometry as the two methods are complementary. Traditional applications are in security screening for explosives and chemical warfare agents as well as for the detection of illicit drugs.^{1–3} Increasingly, the method is also employed for other applications such as food quality control^{4,5} and environmental analysis.^{6,7}

The typical instruments as produced by commercial manufacturers are employed for volatile analytes and consist of a radioactive source for ionization (e.g., ⁶³Ni), an ion shutter for injection of a swarm of ions, alternately stacked electrode (metallic), and insulator rings to form the drift tube for ion separation and a Faraday detector.¹ The construction of such an instrument is considerably less demanding than that of a chromatograph or mass-spectrometer. Therefore, the in-house building of IMS instruments is possible. This may allow wider access to the technique, in particular, for laboratories with financial constraints. Several

developments, some of these only reported in recent years, further facilitate this. The traditional radioactive ionization sources, while simple, require special precautions and permits. Alternatives are, for example, corona discharges,^{8,9} UV-photoionization,^{10–13} low-temperature plasmas,^{14–16} and electrospray ionization (ESI).^{17,18} The latter method is of particular interest as it allows the analysis of liquid samples and, therefore, broadens the scope of applications, while the setup remains simple. The use of printed circuit board material as used for electronic circuitries simplifies the creation of drift tubes and eliminates the need for stacking of rings. As the manufacturing processes are identical to those employed in the electronics industry, the materials can be ordered with the required electrode patterns from printed circuit board supply houses.¹⁸ Drift tubes with rectangular cross sections can be created by using printed circuit board material bearing electrode tracks as the walls as reported by Eiceman *et al.*¹⁹ and by Bohnhorst co-workers.^{20,21} As introduced by Smith *et al.*²² and by our group,¹⁷ drift tubes with the usual circular cross section can be created by rolling up flexible printed circuit board material based on polyimide.

The traditional Bradbury–Nielsen²³ and Tyndall–Powell²⁴ ion gates employed for drift-tube IMS usually consist of two sets of thin wires stretched across the channel. In the former arrangement, the two sets are usually in the same plane, while in the latter case, these

are offset by a short distance between 0.01 and 1 mm.¹ Ion gating is achieved by pulsing the voltage applied to these electrodes for a duration of typically 200 μ s. The construction, especially of the Bradbury–Nielsen gate, is difficult due to the required precision. Zimmermann and co-workers^{25,26} introduced an alternative three-grid shutter based on etched grids rather than a wire mesh. The use of such grids is a further simplification in view of building IMS instruments as these grids can be ordered to the desired design from manufacturers specializing in photochemical micromachining.¹⁸

One of the more significant challenges to overcome when building a drift-tube IMS instrument is the electronic pulser needed for the ion shutter. This requires the fast switching of a voltage of perhaps 50–100 V riding on top of the constant drift tube voltage of typically 5 kV. This is not trivial, and intriguingly, details on the circuitries are generally absent from the experimental sections of publications in the field. Clowers and co-workers state that “these electronics have relied on custom-made, wire-wound isolation transformers” and “have remained either proprietary in nature or custom built from in-house electronics experts.”²⁷ In the spirit of promoting open-source hardware, these authors published the details of a pulse circuitry²⁷ and made the design files available on GitHub (<https://github.com/bhclowers/OS-IMS>) so that they may be duplicated by interested parties. It is also commercially available (www.mstar2k.com/gaace-home). This pulser is based on a floating circuitry, which is tied to the high voltage of the drift tube. It is capable of fast switching of voltages up to 200 V by using high-voltage field-effect transistors (FETs). To allow the floating of the entire circuitry to high voltages, it is isolated from the rest of the circuitry and, therefore, powered by a dedicated, also floating, power source in the form of rechargeable batteries. The trigger signal for the pulses is provided via a fiber optic cable in order to maintain the electrical insulation to the control circuitry.

Herein, an alternative high voltage switching circuitry based on a fast high-voltage optocoupler is reported. It is not based on floating circuitry, i.e., it does not require isolated batteries as a power supply for its own operation. The circuitry has a very low overall electronic component count and is inherently robust.

II. EXPERIMENTAL

A. Pulser electronics and characterization

The high voltage opto-coupler (OPTO-150) is a product of HVM Technology (New Braunfels, TX, USA). As a high voltage source, a module from XP Power (CB101, Pangbourne, UK) is used (but as discussed below, for some tests, a Spellman supply, CZE1000R, Spellman, Hauppauge, NY, USA, was employed). The field-effect transistor (BS170) is a product of ON Semiconductor (Phoenix, AZ, USA). The resistors for the voltage divider, a 2 M Ω trimmer (Bourns 3296Y) and a 50 M Ω high voltage fixed resistor (Murata MHR0424SA506F70), were both obtained from Mouser Electronics (Mansfield, TX, USA). The transient high-voltage measurements on the pulser circuitry were carried out with a 1000:1 high voltage oscilloscope probe (P6015A from Tektronix, Beaverton, OR, USA) with an impedance of 100 M Ω connected to a PC-based oscilloscope connected via a USB interface (Picoscope 5442D, Picotech). The high-voltage measurements on the resistor

ladder of the instrument could only be done in a static mode (because the input impedance of the oscilloscope probe was not adequate). These were performed with a 1000:1 high voltage probe (Testec TT-HVP 40, obtained from Farnell, Zug, Switzerland) with an impedance of 1000 M Ω connected to a multimeter (Fluke 175, Fluke, Everett, WA, USA).

B. Ion mobility spectrometer

A schematic diagram of the electrospray ion mobility spectrometer built in-house is shown in Fig. 1. It essentially consists of an electrospray generator, desolvation tube, ion shutter, drift (separation) tube, detector, and control and measurement electronics. The electrospray was created with a fused silica capillary of 50 μ m inner and 375 μ m outer diameter (TSP-050375-M-10, BGB Analytik AG, Bökten, Switzerland). A syringe pump (KDS 100 legacy, KD Scientific, Holliston, MA, USA) was used to push the solutions through the capillary. The capillary tip was positioned at the entrance of the desolvation section of the IMS instrument with the use of additional custom-made holders. A three-way connector from LabSmith (T-piece T116-203, Livermore, CA, USA) was employed to connect the high voltage for electrospray ionization from a high-voltage generator (CZE1000R, Spellman, Hauppauge, NY, USA).

The instrument itself was based on the open-source hardware design reported by Reinecke and Clowers,¹⁸ but with some adaptations as reported previously.¹⁷ This concerned mainly the use of desolvation and separation tubes made from the flexible printed circuit board material.¹⁷ Two 10 cm wide flexible printed circuit boards with 1.6 mm wide electrodes at a spacing of 2 mm were manufactured in-house with a standard printed circuit board processing protocol, and these were rolled up to form the desolvation and separation drift tube sections. 1 M Ω high voltage surface mount resistors (\pm 1%, HVCB1206FKC1M00, from Stackpole Electronics, Raleigh, NC, USA) were soldered directly onto the ends of the electrode tracks to form the resistor ladder, which creates the drift field. A second Spellman CZE1000R unit was employed as the source of the separation voltage. Nitrogen (N_2) gas (99.999% purity, PanGas, Pratteln, Switzerland) was employed as the drift gas, and its

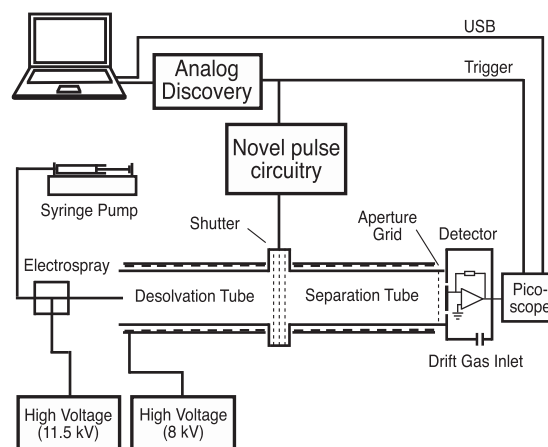


FIG. 1. Schematic drawing of the IMS setup.

flow rate was set with a mass-flow controller (F-201CV-500-ADD-22-V, Bronkhorst, Aesch, Switzerland). The ion shutter consisted of three 100 μm thick etched metal grids of the design reported by Reinecke and Clowers¹⁸ (Newcut, Newark, NY, USA) with 300 μm thick PTFE spacers.

A Faraday plate fitted with an aperture grid identical to the shutter grids was employed for ion detection. The ion currents were measured with a two-stage transimpedance amplifier based on LMC6001 and OPA227P operational amplifiers (both Texas Instruments, Dallas, TX, USA) with an overall amplification of 1.0×10^9 V/A. The signal voltage was recorded with a 16-bit resolution PC oscilloscope (Picoscope 4262, from Picotech, St. Neots, UK) to obtain the mobility spectra. The sequencing of the ion injection and measurements was controlled with an Analog Discovery 2 personal computer-based multifunction unit (Digilent, Pullman, WA, USA).

The reduced mobilities, K_0 , and resolving powers, R_p , were calculated according to the following equations:

$$K_0 = (L/t_d \cdot E) \cdot (p/p_0) \cdot (T_0/T), \quad (1)$$

where L is the length (cm) of the drift tube, E is the field strength (V/cm), t_d is the drift time (s), p and p_0 are the drift tube pressure and standard pressure (760 Torr), respectively, and T and T_0 are the drift tube temperature and standard temperature (273.15 K), respectively,

$$R_p = (t_d/W_{1/2}), \quad (2)$$

where t_d is the drift time (s) and $W_{1/2}$ is the full width at half maximum height (FWHM).

C. Chemicals

The standards tetraethylammonium bromide (T2), tetrabutylammonium bromide (T4), tetrahexylammonium bromide (T6), and tetraoctylammonium bromide (T8) were purchased from Sigma-Aldrich (Buchs, Switzerland). Methanol of the chromatography grade (HiPerSolv, VWR Chemicals, Schlieren, Switzerland) and water purified with a Milli-Q system from Millipore (Bedford, MA, USA) were employed as solvents. A solution of the standards at 5 μM each was prepared in a 50% (v/v) mixture of water and methanol.

III. RESULTS AND DISCUSSION

A. Pulser design

A schematic diagram of the simple gate trigger circuitry based on the OPTO-150 optocoupler is shown in Fig. 2. This optical device is a special product designed for high voltages and is contained in a hermetically sealed opaque case ($0.4 \times 0.24 \times 0.25$ in³) providing rated insulation of up to 15kV. Switching between the two required high-voltage levels is achieved with a voltage divider in which one of its two legs can be shunted by the photodiode contained in the optocoupler. Bypassing the high voltage side resistor causes the voltage to the shutter grid to rise to the full value, i.e., the closed state of the ion shutter. This is achieved with a control signal from the

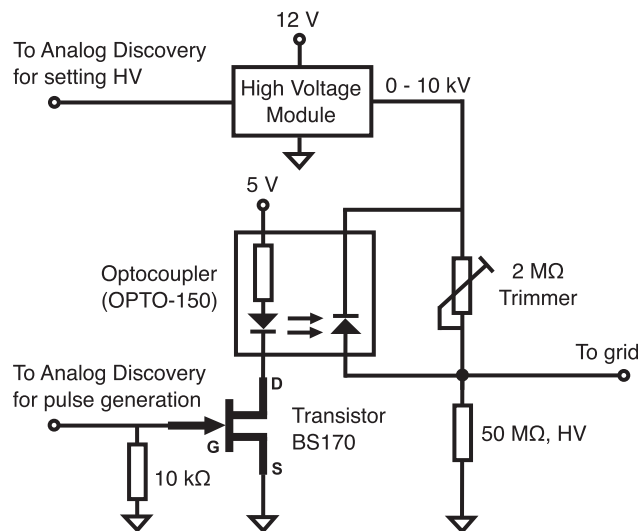


FIG. 2. Circuit diagram of the pulser circuitry based on a fast high-voltage optocoupler. The full voltage of the high-voltage unit is passed to the grid when the photodiode in the optocoupler is made conducting by turning on the LED, while the voltage is reduced when the LED is off as the two resistors form a voltage divider.

low voltage side of the circuitry. The photodiode is conducting when the light-emitting diode (LED) in the optocoupler is turned on with a control signal via a low-power field-effect transistor (FET). The optical coupling provides the insulation of the driving circuitry from the high voltage. The voltage remains at the upper level as long as the LED remains lit. The duration of the pulse is defined by the circuitry providing the control signal. In our case, the digital output of an Analog Discovery multifunction instrument was employed, and the pulse duration was set in its software running on a personal computer. Any other setup providing a pulsed control signal is suitable.

The circuitry requires a precise high-voltage power source. An inexpensive auxiliary high voltage module (XP Power CB101), which can be soldered directly onto the printed circuit board of the pulser circuitry, was employed. This is a regulated unit whose output voltage (up to a maximum of +10 kV) is set with an analog control voltage between 0 and 5 V. This allows the setting of the upper level of the gate voltage for the closed state. In our case, the control voltage was provided by an analog output of the Analog Discovery multifunction instrument (with a 14-bit digital-to-analog converter), and therefore, could also be set in software, but if it does not need to be flexible a fixed control voltage could be provided. The output voltage was measured using a high voltage probe and a high-resolution multimeter. The drop in voltage for opening the gate can be adjusted by changing the resistance of the upper leg of the voltage divider. This is achieved by using a trimmer resistor of 2 M Ω . In this work, about 50 V was employed, but this may easily be adapted by using resistors of different values. The lower leg was a high-voltage resistor with a value of 50 M Ω , except where stated otherwise. The circuitry requires a 12 V supply to power the high-voltage module and a 5 V supply for the LED of the optocoupler. The ground of the pulser

circuitry is tied to the ground of the main circuitry (consisting of the high-voltage supply for the drift tubes and the control and data-acquisition sections). Note that the input side of the optocoupler does not require an external current limiting resistor when driven at 5 V as it features a built-in current limiting resistor. The pulser device was built on a generously laid out printed circuit board and housed in a non-metallic case to provide safety insulation.

B. Pulse characteristics

In drift-tube IMS, injection times are typically in the range from 100 to 400 μs .¹ Therefore, the pulse circuitry has to have switching times faster than this, as otherwise a significant distortion of the pulse would lead to a bias in the injection of the ions. The output of the new circuitry for an injection pulse by temporarily switching from 4025 to 3980 V is illustrated in Fig. 3(a). Note that the oscilloscope probe adds an additional load due to its limited input impedance (100 M Ω). The current drawn with the original load resistor of 50 M Ω in the circuitry (the lower leg of the voltage divider) would then exceed the maximum output current of 100 μA of the high-voltage module. For the purpose of this measurement, the resistor in the circuitry was, therefore, changed from 50–100 M Ω . The total load resistance (2 resistances of 100 M Ω in parallel) for the measurement, thus corresponded to the original 50 M Ω without the presence of the probe. The fall and rise times indicated as 15.7 and 2.0 μs , respectively, in the plot were determined by a built-in software routine of the PC-based oscilloscope as the times between 10% and 90% of the voltage change. These times are deemed to be adequate for the typical injection times of IMS. The delays must be caused by the junction capacitance of the photodiode. The fact that the fall time is slower than the rise time can be rationalized by a discharge of the junction capacitance through the resistor forming the lower leg of the voltage divider. This was confirmed by carrying out further tests with different resistors for the lower leg of the voltage divider as given in Fig. 3(b). Note that these measurements were carried out with one of the Spellman high-voltage power supplies, rather than the module used in the pulser circuitry (CB101), due to their higher maximum output current. Clearly, the resistance has a strong influence on the fall times, and lower resistances lead to faster responses, while the effect on the rise times is much less pronounced. Therefore, the fall time may be minimized by employing a high voltage module with a higher current capability and using lower resistance values, as long as the current limit of the photodiode in the optocoupler of 400 μA is not surpassed. Note that the slight slant at the bottom of the pulses. The reason for this is not known, but it is not expected to significantly affect the performance.

C. Field-switching at the three-grid shutter

The novel pulse circuitry was demonstrated with the three-grid field switching shutter, which is part of the open-source hardware IMS design¹⁸ adopted by us,¹⁷ but is, in principle, also suitable for Tyndall-Powell shutters. The setup of the three-grid shutter is shown schematically in Fig. 4. Grid electrode 1 and grid electrode 3 are made part of the voltage divider ladder defining the electric field, which is driving the ions through the desolvation and drift tubes toward the detector. These grids are directly in contact with the

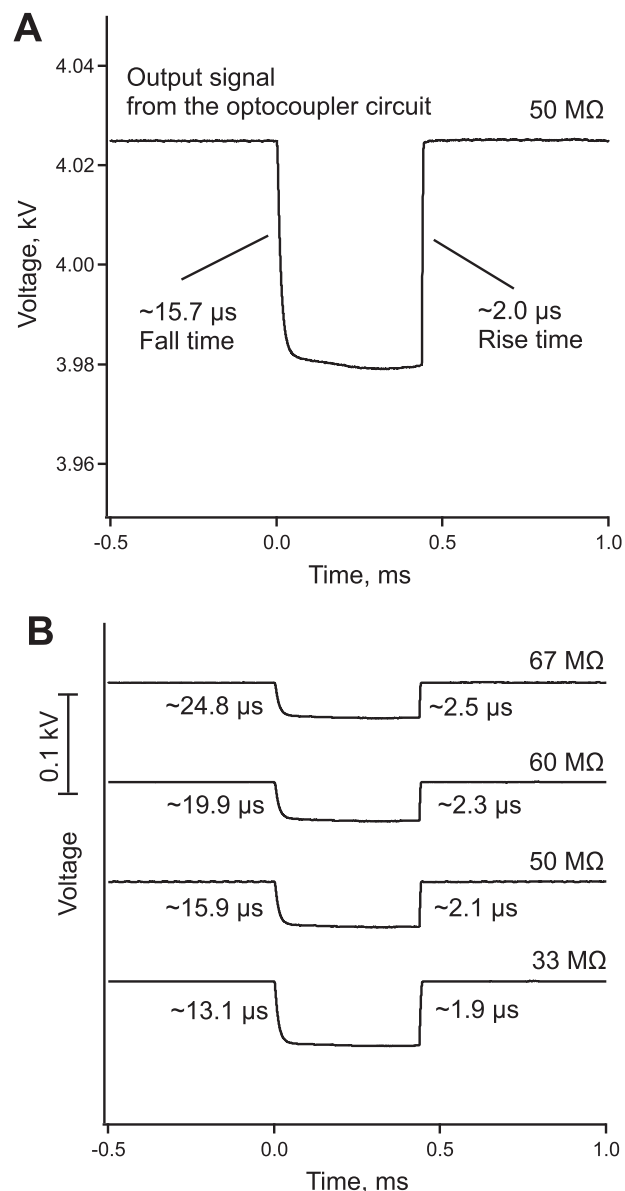


FIG. 3. (a) Pulse output of the circuitry with the 50 M Ω load resistance as the lower leg of the voltage divider. (b) Effect of load resistance on the fall and rise time of the pulse, determined with the Spellman (CZE1000R) high-voltage power supply.

last and first ring electrodes of the desolvation and separation tubes, respectively, and are bridged with a gate resistor of 300 k Ω in order to obtain a voltage drop between the two outer grid electrodes, which is equivalent to the field strength along the drift tube. To stabilize the voltages on these electrodes, they were fitted with buffer capacitors of 4.7 nF (10 kV). The grid electrode in the center (grid electrode 2) is not connected to the voltage ladder. Its voltage is determined independently by the new pulser circuitry in order to block or admit the passage of the ions. The two outer grids minimize a disturbance

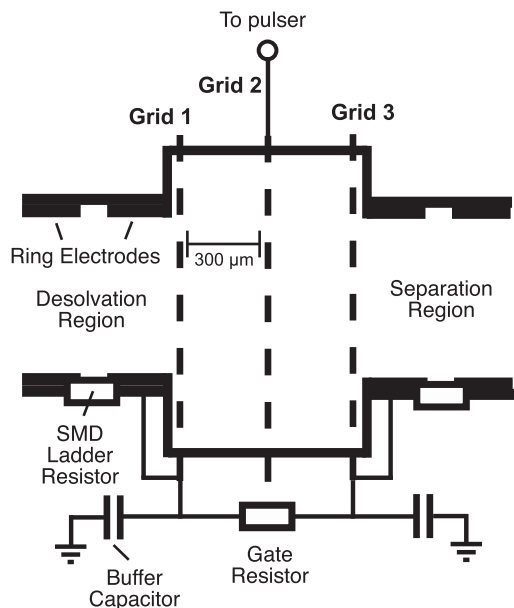


FIG. 4. Arrangement of the three-grid shutter showing the electrical connections (not to scale). Grid 1 and grid 3 are connected to the last and first ring electrodes of the drift tubes and bridged with the gate resistor, while grid 2 is driven independently by the pulser circuitry.

of the electric fields in the desolvation and separation sections of the drift tube when the shutter is closed by the adjustment of the potential of the central shutter electrode (grid 2).²⁸

The voltages measured across the three-grid shutter and at the second ring electrode of the separation drift tube as well as the second to last ring electrode of the desolvation tube, when applying the closing and opening potentials, are shown in Fig. 5(a). In the closed state, the voltage at grid 2 is higher than at grid 1, creating a reversed field and a barrier for the ions. In the open state, the voltage at grid 2 is at the mean between the two outer grids enabling the ions to migrate through the shutter before entering the separation drift tube for analysis. As expected, the voltages at the outer grid electrodes and the adjacent ring electrodes were not affected when changing the potential at the center electrode. The dynamic behavior is illustrated schematically in Fig. 5(b).

D. Performance

The characterization of the performance of the instrument with the new pulser circuitry is shown in Fig. 6. Four quaternary amines were injected as model analytes, and the effect of the injection time ranging from 100 to 600 μs was studied using the operating parameters given in Table I. As expected, the mobility spectra shown in Fig. 6(a) show a strong increase in peak intensity with injection time. The quantitative data are shown in Fig. 6(b) in the form of the peak area vs injection time for one of the compounds (T8 = tetraoctylammonium). On the other hand, the resolving power, R_p , is also dependent on the injection time and for T8 was found to deteriorate from about 85 to 62 on increasing the injection time from

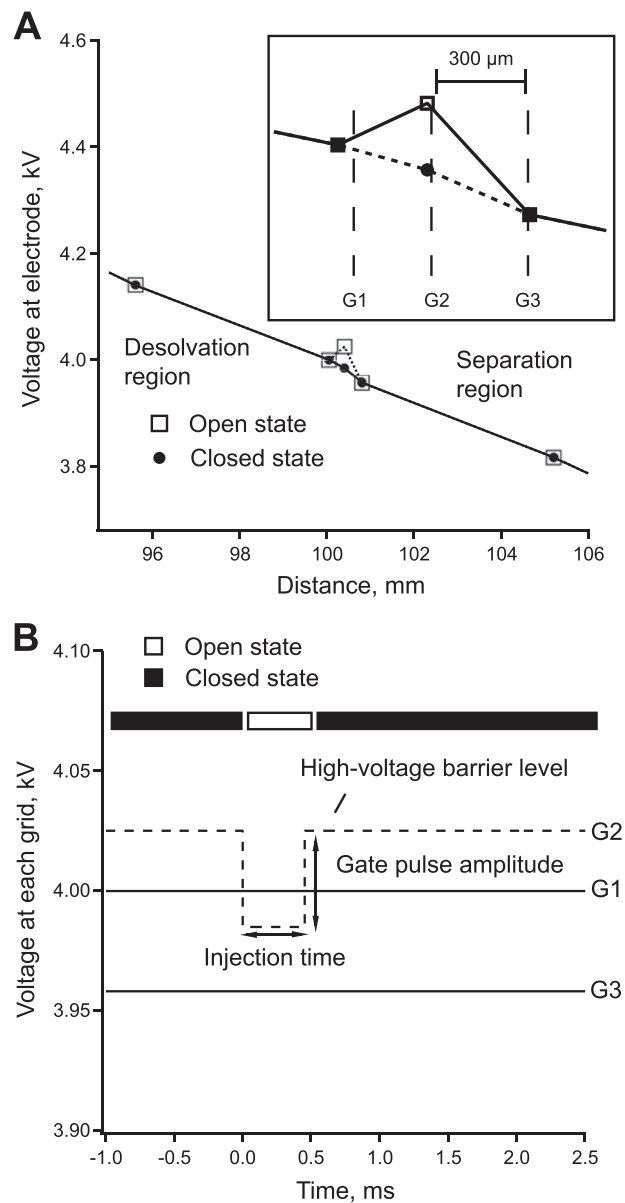


FIG. 5. (a) Voltages measured at the three-grid electrodes and the adjacent ring electrodes for the closed and open shutter states with an insert focusing on the grid electrodes. (b) Schematic representation of the pulsing regime.

200 to 600 μs . Because of the improved resolving power, short injection times are, in principle, preferable, but due to the loss of sensitivity, this can only be made use of to a limited extent. Note that the resolving power is also dependent on diffusion and space charge effects, as well as the nature of the ion detected and the applied field strength.²¹ As a compromise between resolving power and sensitivity, an injection time of 450 μs was adopted, which still gives a resolving power over 75. This can be considered state of the art.²¹ For this gate opening time and otherwise identical conditions,

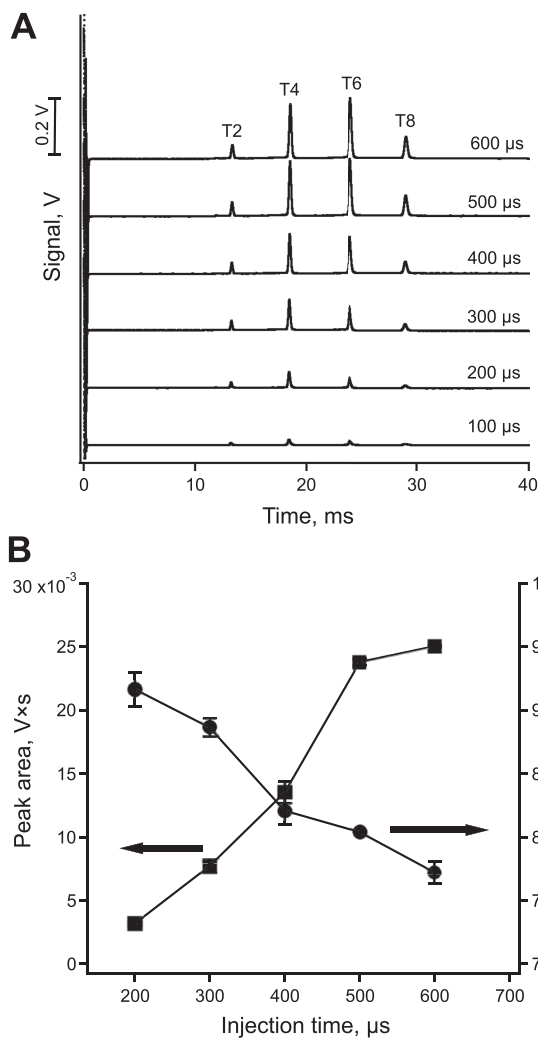


FIG. 6. (a) Mobility spectra for a mixture of tetraethylammonium (T2), tetrabutylammonium (T4), tetrahexylammonium (T6), and tetraoctylammonium (T8) ($5 \mu\text{M}$ each) obtained for different injection times between 100 and $600 \mu\text{s}$. (b) Plots of the peak area and resolution for different injection times for T8.

a 1:1 comparison was also carried out with the previously employed pulser circuitry. This is the floating FET-based pulser reported by Garcia *et al.*²⁷ discussed in the Introduction. Resolving powers of over 70 had been reported for IMS instruments employing this pulser.^{17,18}

The two spectra are shown in Fig. 7. As can be seen, very similar results were obtained, and this confirms that the new pulser performs as well as the reference design. However, the peaks for the optocoupler pulser were just slightly taller. The reason for this is not known. The numerical performance data obtained with the two pulsers using the identical settings are summarized in Table II. As expected, very similar results were obtained for the drift times and, therefore, the reduced mobilities but also for the resolving powers.

TABLE I. Operating parameters of the IMS instrument and its injection gate.

Electrospray ionization	
Flow rate ($\mu\text{L}/\text{min}$)	0.8
ID of the capillary (μm)	50
OD of the capillary (μm)	375
Length of the capillary (cm)	5.0
Electrospray voltage (kV)	11.5
Injection gate	
Injection time (μs)	100–600
Gate high voltage (kV)	4.0
Gate pulse voltage (V)	50
Distance between grids (μm)	300
Gate resistor (k Ω)	300
Drift tube	
Length of the desolvation tube (cm)	10.0
Length of the separation tube (cm)	10.0
Field strength (V/cm)	400
Electrode width (mm)	1.6
Spacer gap (mm)	2.0
N ₂ drift gas flow rate (ml/min)	500
Drift tube temperature ($^{\circ}\text{C}$)	23 ± 2
Drift tube pressure (Torr)	766 ± 5
Ion detection	
Number of averaged readings (times)	500
Total gain (V/A)	1.0×10^9
Analysis time (s)	50

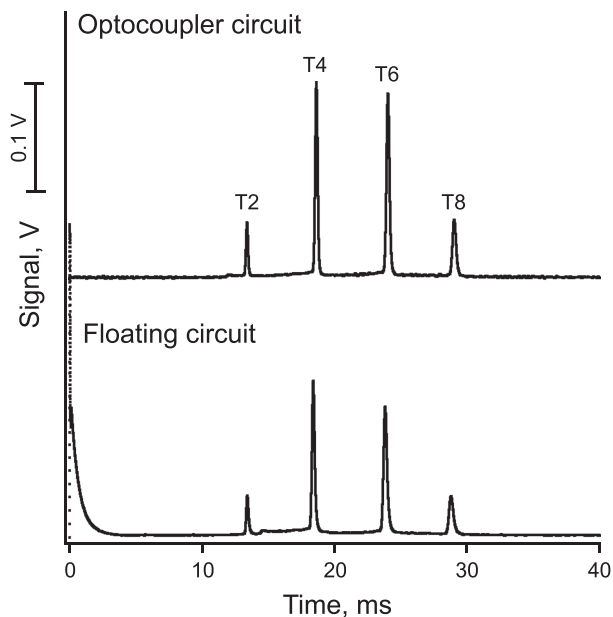


FIG. 7. Comparison of mobility spectra obtained with the new pulser circuitry and the floating pulsing circuitry.

TABLE II. Characteristics of peaks obtained with the two pulsers.

Compound ^a	Optocoupler pulse generator				Floating pulse generator			Reported in literature ²⁸
	Drift time (ms)	Reduced mobility, K_0 (cm ² V ⁻¹ s ⁻¹)	Precision of K_0 (%RSD, n = 5)	Resolving power, R_p	Drift time (ms)	Reduced mobility, K_0 (cm ² V ⁻¹ s ⁻¹)	Resolving power, R_p	Reduced mobility, K_0 (cm ² V ⁻¹ s ⁻¹)
T2	13.4	1.73	0.75	61	13.5	1.72	54	1.73
T4	18.5	1.25	0.27	66	18.4	1.25	63	1.23
T6	24.0	0.97	0.12	75	23.9	0.97	70	0.95
T8	29.0	0.80	0.32	81	28.8	0.80	80	0.78

^aT2, tetraethylammonium; T4, tetrabutylammonium; T6, tetrahexylammonium; T8, tetraoctylammonium.

IV. CONCLUSIONS

The new pulser design based on a fast switching optocoupler led to a performance of the IMS instrument in terms of resolving power that was comparable to that obtained with a previously described pulser. While other types of pulsers may have faster switching times than the new circuitry, this was, therefore, not found to be limiting the performance of the instrument. To our knowledge, this is the first time that such an optocoupler-based pulser has been used for ion injection in ion mobility spectrometry. Its design is simple, and it can be built without special electronics expertise or advanced tools as it does not include any small surface mount devices. As the gate pulsers have been the most intricate part of the electronics in IMS, this facilitates the in-house construction of IMS instruments, thus making the method more widely available in the spirit of open-source analytical hardware. The optocoupler-based pulser can also readily be adapted to anion IMS. Furthermore, with some modifications, it should also be possible to make use of the high voltage source employed to power the drift tube instead of requiring a separate high voltage module.

ACKNOWLEDGMENTS

The authors acknowledge the financial support from the Development and Promotion of Science and Technology Talents Project of Thailand (Grant No. DPST 532133).

AUTHOR DECLARATIONS

Conflict of Interest

The authors have no conflicts to disclose.

Author Contributions

Nattapong Chantipmanee: Investigation (equal); Writing – original – draft (equal). **Marc-Aurèle Boillat:** Investigation (equal). **Peter C. Hauser:** Conceptualization (equal); Supervision (equal); Writing – original – draft (equal); Writing – review & editing (equal).

DATA AVAILABILITY

The data which support the findings of this study are available within the article.

REFERENCES

- G. A. Eiceman, Z. Karpas, and H. H. Hill, *Ion Mobility Spectrometry* (CRC Press, Boca Raton, 2013).
- M. A. Mäkinen, O. A. Anttalainen, and M. E. T. Sillanpää, *Anal. Chem.* **82**, 9594 (2010).
- J. Puton and J. Namiěšnik, *TrAC Trends Anal. Chem.* **85**, 10 (2016).
- M. Hernández-Mesa, D. Ropartz, A. M. García-Campaña, H. Rogniaux, G. Dervilly-Pinel, and B. Le Bizec, *Molecules* **24**, 2706 (2019).
- Z. Karpas, *Food Res. Int.* **54**, 1146 (2013).
- I. Márquez-Sillero, E. Aguilera-Herrador, S. Cárdenas, and M. Valcárcel, *TrAC Trends Anal. Chem.* **30**, 677 (2011).
- S. Armenta, F. A. Esteve-Turrillas, and M. Alcalá, *Anal. Methods* **12**, 1163 (2020).
- C. A. Hill and C. L. P. Thomas, *Analyst* **128**, 55 (2003).
- M. Tabrizchi, T. Khayamian, and N. Taj, *Rev. Sci. Instrum.* **71**, 2321 (2000).
- C. Chen, D. D. Jiang, and H. Y. Li, *Anal. Chim. Acta* **1077**, 1 (2019).
- N. Chantipmanee and P. C. Hauser, *Int. J. Ion Mobility Spectrom.* **23**, 161 (2020).
- D. Young, K. M. Douglas, G. A. Eiceman, D. A. Lake, and M. V. Johnston, *Anal. Chim. Acta* **453**, 231 (2002).
- M. A. Chavarria, A. V. Matheoud, P. Marmillod, Y. Liu, D. Kong, J. Brugger, and G. Boero, *Rev. Sci. Instrum.* **88**, 035115 (2017).
- H. Hayen, A. Michels, and J. Franzke, *Anal. Chem.* **81**, 10239 (2009).
- M. T. Jafari, *Anal. Chem.* **83**, 797 (2011).
- N. Chantipmanee, J. S. Furter, and P. C. Hauser, *Anal. Chim. Acta* **1195**, 339432 (2022).
- N. Chantipmanee and P. C. Hauser, *Anal. Chim. Acta* **1170**, 338626 (2021).
- T. Reinecke and B. H. Clowers, *HardwareX* **4**, e00030 (2018).
- G. A. Eiceman, H. Schmidt, J. E. Rodriguez, C. R. White, E. V. Krylov, and J. A. Stone, *Instrum. Sci. Technol.* **35**, 365 (2007).
- A. Bohnhorst, A. T. Kirk, and S. Zimmermann, *Int. J. Ion Mobility Spectrom.* **19**, 167 (2016).
- A. Bohnhorst, A. T. Kirk, and S. Zimmermann, *Anal. Chem.* **93**, 6062 (2021).
- B. L. Smith, C. Boisdon, I. S. Young, T. Praneenararat, T. Vilaivan, and S. Maher, *Anal. Chem.* **92**, 9104 (2020).
- N. E. Bradbury and R. A. Nielsen, *Phys. Rev.* **49**, 388 (1936).
- A. M. Tyndall and C. F. Powell, *Proc. R. Soc. London, Ser. A* **129**, 162 (1930).
- J. Langejuergen, M. Allers, J. Oermann, A. Kirk, and S. Zimmermann, *Anal. Chem.* **86**, 7023 (2014).
- J. Langejuergen, M. Allers, J. Oermann, A. Kirk, and S. Zimmermann, *Anal. Chem.* **86**, 11841 (2014).
- L. García, C. Saba, G. Manocchio, G. A. Anderson, E. Davis, and B. H. Clowers, *Int. J. Ion Mobility Spectrom.* **20**, 87 (2017).
- T. Reinecke, A. T. Kirk, A. Ahrens, C.-R. Raddatz, C. Thoben, and S. Zimmermann, *Talanta* **150**, 1 (2016).